where fewer such internal sites exist (needle coke) and transport of the carbon particle to "external" sites is responsible for a significant fraction of the catalysis. External mass transport rate control would also account for the apparent insensitivity to catalyst type of the rate enhancement observed for needle coke burning in the presence of separate catalyst particles.

Conclusions

The burning rates of "dry" petroleum cokes (i.e., cokes which are free of residual oil volatiles) having similar initial surface areas are not influenced by process origin (delayed vs fluid coking). Differences in burning rate among the coke samples tested are related to the native metals level in the coke which can exert a catalytic influence on the burning rate. This effect diminishes with increasing temperature as higher activation energy thermal reactions begin to dominate.

The addition of separate particles of low surface area catalytic solids can accelerate the combustion of petroleum coke and similar carbonaceous residues. The extent of the rate enhancement from an external catalyst declines with increasing temperature and increasing native metals content of the solid fuel. Moreover, these findings suggest that the primary benefit from separate particle catalysis in practical fluid bed combustors for steam generation would be enhanced conversion of CO to CO_2. Finally, the comparative insensitivity of the rate enhancement to catalyst type and the low apparent activation energies observed are both qualitatively consistent with a rate-limiting step involving transport of coke particles to the surface of the separate catalyst particles.

Literature Cited

Buch, T.; Guala, J. A.; Caneiro, A. *Carbon* 1978, *16*, 377.
Chester, A. W.; Schwartz, A. B.; Stover, W. A.; McWilliams, J. P. *CHEMTECH* 1981, *11*, 50.
Gutfinger, C.; Tardos, G. I. *Atm. Environ.* 1979, *13*, 853.
Hougen, O. A. *Ind. Eng. Chem.* 1961, *53*(7), 509.
Juntgen, H. *Fuel* 1983, *62*, 234.
Laurendaen, N. M. *Prog. Energy Combust. Sci.* 1978, *14*(4), 221.
Marsh, H.; Adair, R. R. *Carbon* 1975, *13*, 327.
McKee, D. W. "Mechanisms of Catalyzed Gasification of Carbon". Report 80CRD143, 1980; General Electric Corporate Research and Development.
McKee, D. W. In *Chemistry and Physics of Carbon*; Walker, P. L., Jr., Thrower, P. A., Eds.; Marcel Dekker: New York, 1981; Vol. 16, pp 1–118.
McKee, D. W.; Spiro, C. L.; Kosky, P. G.; Lamby, E. J. *Fuel* 1983, *62*, 217.
Mulcahy, M. F. R.; Smith, I. W. *Rev. Pure App. Chem.* 1969, *19*, 81.
Smith, I. W. *Fuel* 1978, *57*, 409.
Tyler, R. J. *Fuel* 1986, *65*, 235.
Walker, Jr., P. L.; Rusinko, F., Jr.; Austin, L. G. *Adv. Catal.* 1959, *11*, 133.
Weisz, P. B.; Goodwin, R. D. *J. Catal.* 1966, *6*, 227.

An Investigation of Reaction Pathways and Reaction Kinetics for the Liquid-Phase Catalytic Amination of Long-Chain Alkenals by the Use of a Model Compound

Patrick L. Mills,* Donald E. Willis, and Ricky L. Fenton

Monsanto Company, Central Research Laboratory, 800 North Lindbergh Boulevard, Q3B, St. Louis, Missouri 63167

The liquid-phase reductive amination of a novel class of long-chain substituted 2-alkenals by dimethylamine and hydrogen in the presence of various heterogeneous catalysts is examined. The reaction characteristics of these alkenals are investigated by use of a single isomer that mimics the key chemical features of the remaining isomers in the mixture. A novel gas chromatographic method is used to resolve and identify all stable reaction intermediates from which the reaction pathways, reaction thermodynamics, and reaction kinetics are determined. Typical supported base metal catalysts, such as those containing cobalt, nickel, and copper, are shown to promote the formation of long-chain alcohols which are undesired side products. Use of a carbon-supported palladium catalyst gives high selectivity to the desired saturated amine product at a temperature and pressure not exceeding 373 K and 3551 kPa, respectively. Comparisons between the reaction rates for the reductive amination of the alkenal isomer with dimethylamine to those reported in the literature for the reductive amination of a long-chain alcohol show that the former one proceeds at significantly lower temperatures at rates that are nearly 2 orders of magnitude greater than those for the alcohol amination.

Long-chain aliphatic amines are important chemical intermediates that are used to synthesize a wide variety

of commercial products. They are perhaps best known for their use in various applications where it is desired to alter the interfacial or surface active properties of a liquid medium by formation of basic and cationic species (Bathina and Reck, 1978). Because of their industrial significance, numerous process-oriented routes have been

---

*Author to whom correspondence should be addressed. Present address: Department of Chemical Engineering, Washington University, Campus Box 1198, St. Louis, MO 63130.
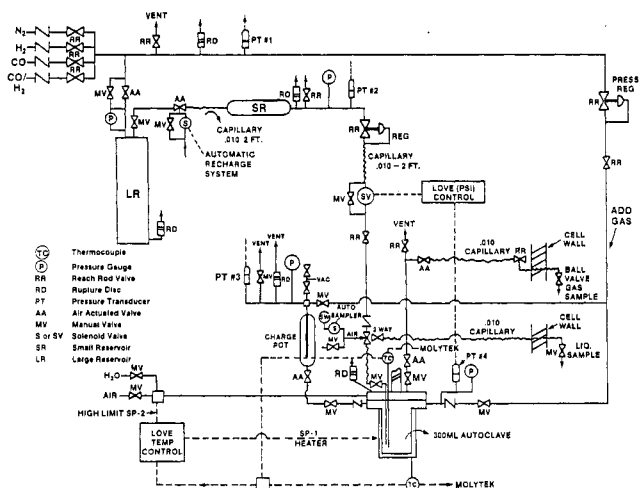
Figure 1. High-pressure autoclave reactor system used for the reactant synthesis and reductive amination reaction experiments.

proposed for the selective synthesis of long-chain amines (Beil et al., 1969; Dadekian and Wilbourn, 1969; Dudzinski, 1970, 1973; Hoshino et al., 1980; Imai, 1979, 1980, 1981; Kimura et al., 1981; Kraiman and Austin, 1968; Mather et al., 1979; McCarty et al., 1969; Mueller et al., 1977; Pivette, 1973; Slaugh, 1980a, 1980b, 1982; Strauss et al., 1979; Wakeman and Shay, 1969; Wattimena et al., 1979). The amine products and their derivatives described in these routes are mostly well-known derivatives of ammonia in which one or more of the hydrogen atoms are replaced by alkyl groups having greater than six carbons. In addition, the emphasis of the invention is typically placed upon development of an alternate method for preparing a known amine which has some claimed process advantage over previous approaches.

Many of the direct methods cited above for the synthesis of long-chain amines involve gas–liquid–solid catalyzed reactions between linear aldehydes, alcohols, or ketones with hydrogen as the reducing agent and either ammonia or short-chain primary and secondary amines having less than six carbons as the nitrogen source. Certain fundamental and practical aspects associated with the catalysis of these systems that are useful in heterogeneous reactor design and other related applications have been discussed in various review papers (Baiker and Kijenski, 1985; Herman, 1984; Klyuev and Khidekel, 1980; Nekrasova and Shuikin, 1965) and a monograph (Rylander, 1979). While some generalizations on issues such as selection of the optimal catalyst type, catalyst deactivation, reaction conditions, reaction pathways, reaction mechanisms, and reaction kinetics for amination of the above classes of compounds can be made, data are still fragmentary and do not yet exist for many systems that might be of interest. For example, the reaction kinetics and reaction pathways for the reductive amination of certain long-chain alcohols were just recently studied (Baiker et al., 1983) with more broad coverage of other topics being given in a review (Baiker and Kijenski, 1985).
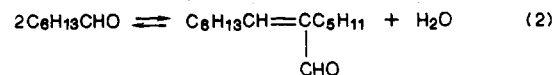
An indirect route for the synthesis of long-chain amines that have novel compositions has recently been proposed (Forster et al., 1986). In one proposed route, a mixture of C_6 hexene isomers, such as those obtained by propylene dimerization (Weissermel and Arpe, 1978), are converted to a mixture of C_7 aldehyde isomers using a homogeneous cobalt catalyst in an oxo hydroformylation process (Falbe, 1980). These aldehydes, which predominantly consist of various isomers with no substituent group in the carbon 2 position, are then subjected to an aldol condensation to

produce C_{14} unsaturated aldehydes with at least one main branch in the 2 position, i.e., 2-alkenals. Reductive amination of the 2-alkenals using either ammonia or primary or secondary short-chain amines yields a mixture of long-chain amines in which each species in the mixture represents a novel compound. A typical example of the chemical reactions associated with each of these steps is given below for the case where dimethylamine is used as the short-chain amination reagent.
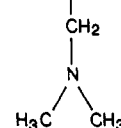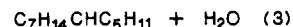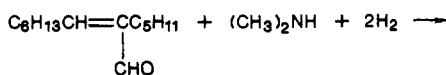
oxo hydroformylation of hexenes

$$C_6H_{12} + CO + H_2 \longrightarrow C_6H_{13}CHO \qquad (1)$$

aldol condensation of aldehydes

$$2C_6H_{13}CHO \rightleftharpoons \underset{\underset{CHO}{|}}{C_6H_{13}CH{=}CC_5H_{11}} + H_2O \qquad (2)$$

reductive amination of alkenals

$$\underset{\underset{CHO}{|}}{C_6H_{13}CH{=}CC_5H_{11}} + (CH_3)_2NH + 2H_2 \longrightarrow$$

$$\underset{\underset{\underset{\underset{H_3C\diagup\diagdown CH_3}{N}}{|}}{CH_2}}{C_7H_{14}CHC_5H_{11}} + H_2O \qquad (3)$$

The above sequence assumes that the final desired product is the long-chain saturated amine whose general formula is given in eq 3. The situation where the mixture of isomeric amine products contains a certain fraction that has internal unsaturation represents another possibility. For the product applications of this work, however, saturated amines were the desired products. Reductive amination of the unsaturated aldehydes that appear in eq 3 and the various technical aspects associated with the catalysis of this reaction have not been reported. These are of interest to fill an existing gap from both a catalysis as well as a process design and development point of view.

As briefly mentioned above, the scheme given by eq 1–3 was originally proposed with the intention of using a mixture of C_6 hexenes as the carbon source. Process economics evaluations showed that this feedstock yielded a lower manufacturing cost when compared to the case where a single hexene isomer was used. From the standpoint of studying the catalysis and kinetics of the reductive amination reaction given by eq 3, however, use of the C_6 hexene mixture results in a complex mixture of 2-alkenals as the reactant for eq 3 which contains up to 28 distinct isomers. Since the analytical resolution of the individual isomers and potential reaction products derived from them cannot be readily performed on the level required to study their individual reactivity, an alternate approach becomes necessary. The one used here is based upon use of a single 2-alkenal isomer to mimic the behavior of the complete isomer mixture. This is reasonable since the remaining isomers differ only in the type of alkyl groups attached to the carbon 2 position and this part of the molecule does not undergo any chemical transformation during reductive amination.

One objective of the present study is to identify a suitable heterogeneous catalyst for the reductive amination reaction given by eq 3 that leads to the desired amine products in high selectivity which might be considered in a future process development. Another objective is to identify reaction intermediates associated with formation of the long-chain amine and to investigate the possible reaction pathways and reaction thermodynamics. A final objective is to provide quantitative interpretation of a
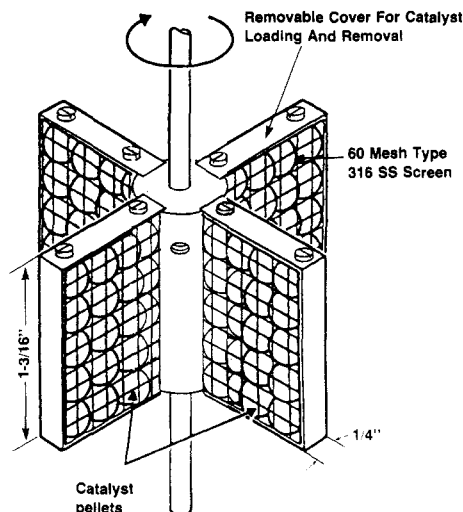
Figure 2. Carberry-type spinning basket used for reaction experiments with catalyst pellets.

typical set of isothermal kinetic data to provide a basis for a future kinetic investigation involving the complex mixture of 2-alkenals.
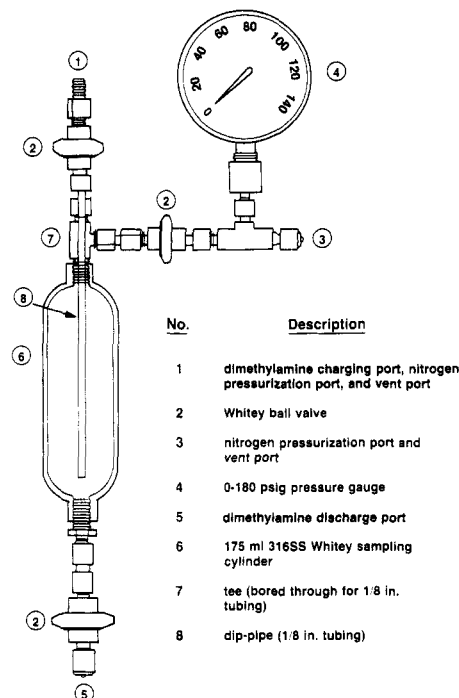
Experimental Section

Apparatus. A diagram of the reaction system that was used to both synthesize the reagents that were not available from commercial sources and to perform the subsequent reductive amination reaction experiments is given in Figure 1. All components were located in a special enclosure with provisions for manual operation of all valves through reach rods to an external panel for operator safety. Synthesis of the model compound 2-pentylnon-2-enal was performed in a 1-gal Autoclave Engineers autoclave, while all reductive amination experiments were performed in a 0.3-L Autoclave Engineers autoclave that was located in a similar enclosure. The latter reactor was operated at a constant gas pressure using a batch liquid and either a powdered or pelleted form of the selected heterogeneous catalyst.

Experiments involving the pelleted catalysts were performed by replacing the six-bladed turbine supplied by Autoclave Engineers with a Carberry-type spinning basket that was specially designed and fabricated to fit within the 0.3-L autoclave. The basket, which is illustrated in Figure 2, could accommodate up to 6.35-mm-o.d. ($^1/_4$-in.) catalyst pellets. It was properly baffled to prevent vortexing and to provide good gas dispersion and liquid–solid mixing. Qualitative visual observation of the gas-bubble mixing pattern was verified in separate experiments using a glass vessel whose internal dimensions matched those of the original reactor vessel.

Both the reactant (hydrogen) and inert gases (argon or nitrogen) were piped to the primary manifold from high-pressure ($P \geq 27\,579$ kPa) laboratory cylinders. The large reservoir (LR in Figure 1) was used to store the reactant gas (hydrogen) in excess of 20 684 kPa. During a reductive amination experiment, hydrogen from this reservoir could be intermittently charged to the small reservoir (SR in Figure 1) by a manually activated air-operated valve. Hydrogen flowed to the reactor from the small reservoir upon demand through a series of valves and a Tescom back-pressure regulator that maintained a constant pressure in the reactor. The gas was introduced to the reaction liquid through a 2-μm porous metal filter that was located below the reactor turbine or basket for good gas dispersion.

Liquid samples could be removed from the reactor during the course of an experiment and analyzed by the

No.	Description
1	dimethylamine charging port, nitrogen pressurization port, and vent port
2	Whitey ball valve
3	nitrogen pressurization port and vent port
4	0-180 psig pressure gauge
5	dimethylamine discharge port
6	175 ml 316SS Whitey sampling cylinder
7	tee (bored through for 1/8 in. tubing)
8	dip-pipe (1/8 in. tubing)

Figure 3. Vessel used for handling and transfer of dimethylamine to the autoclave.

gas chromatographic methods described below. The sampling tubing was selected so that the effect of removing purges and samples on the volume change of the reaction mixture was considered negligible. The sampling line leading from the reactor was connected to a capillary tubing coil that was installed in an ice–water bath downstream of the sample collection valve. This provided sufficient cooling of the hot reaction liquid and reduced flashing as a result of the pressure reduction between the reactor and sample discharge.

The pressures at various locations in the system (small reservoir, large reservoir, and reactor) were monitored by strain gauges that had an absolute accuracy of ±68.9 kPa. Reactor heating was provided by the standard single-zone tubular furnace that was supplied with the autoclave. To prevent temperature drifts and long-term temperature transients caused by the significant thermal capacity of the autoclave body, the average temperature of the reactor outer wall and the liquid batch was used as the control temperature for a PID (Love) temperature controller. In addition, a constant flow of cooling air was maintained through the internal autoclave coils for removal of the heat of reaction and to minimize reactor temperature overshoots. Using this arrangement, the temperature of the batch liquid could be controlled within ±1 K of the desired set point during the course of an experiment.

Due to the significant vapor pressure of dimethylamine at room temperature ($P^* = 232.5$ kPa at $T = 303$ K) and the potential hazards associated with operator exposure to this reactant, a special purpose portable vessel with appropriate valves, transfer lines, and pressure relief, as shown in Figure 3, was used for both containment and charging of this particular reactant. This proved to be an effective method for handling dimethylamine that satisfied safety requirements.

All system components that were in contact with gas or liquid reactants and products were constructed of Type 316 stainless steel. Reactor internals were constructed of Hastelloy C for increased longevity.

Logging of key reaction data, such as the elapsed reaction time, pressures, and temperatures, was performed by

Table I. Properties of Catalysts

catalyst	form	chem composition before reduction, wt %	BET surface area, m^2/g	pore vol, cm^3/g
Engelhard Pd/C	270–325-mesh powder	5% Pd	950	
Harshaw Ni 3210	270–325-mesh powder	36% Ni, balance support	165	0.39
Harshaw Ni-3210	$^1/_8$-in. tablets	36% Ni, balance support	165	0.39
Harshaw Co-0164	$^1/_8$-in. tablets	25% Co, balance support	17	0.50
UCI G-62-Co	270–325-mesh powder	33% Co as Co_3O_4 (unreduced)	52	0.06
Calsicat E-106TR copper chromite	270–325-mesh powder	42% Cu as CuO, 40% Cr as Cr_2O_3, 8% Ba as BaO	90	0.18

using a strip charge recorder (Molytek) with separate LED panel meters. Continuous graphical display with an intermittent printout of key data at a fixed time interval was used.

Materials. Preparation of 2-pentylnon-2-enal was performed by an aldol condensation of n-heptanal which occurs according to the stoichiometry given by eq 2. Methanol was used as a cosolvent to increase the mutual solubility of n-heptanal and hydroxide ion so that acceptable reaction rates and high conversion of reactant could be obtained. All reactants were used as received from commercial sources without additional treatment. In a typical experiment, 803.7 g (1 L at 293 K) of methanol and 1037.7 g (1 L at 293 K) of 1 N aqueous NaOH solution was charged to the 1-gal autoclave through the top port while purging the autoclave with argon. After the top port was installed, the autoclave was pressurized with argon to 689.5 kPa to provide an inert atmosphere, and the reactor contents were agitated for several minutes. The agitation was stopped, and the reactor was slowly vented to atmospheric pressures to remove air from the system. After this procedure was repeated several times, the autoclave contents were slowly heated from 301 to 373 K at 1000 rpm using an argon pressure of about 69.5-kPa gauge. Once the temperature had stabilized, 818.3 g (1 L at 293 K) of n-heptanal was charged to the autoclave from a 4-L Whitey sampling cylinder that was pressurized with argon. The final autoclave pressure after the temperature had stabilized to 376 K was typically about 1862-kPa gauge. After 2 h of reaction time, the reactor was cooled down and the crude product was removed, which readily separated into two liquid phases. The lower (caustic–methanol) phase was discarded, and the top (organic product) phase was washed several times with degassed, distilled water to extract most of the dissolved methanol and hydroxide solution. In one experiment of this type, the washed product was vacuum distilled to remove most of the remaining water, methanol, and any unreacted n-heptanal. Analysis of the combined aqueous washes was performed by gas chromatography using method 1 which is described in a later section. This method, which does not involve derivatization of the sample and is based upon area normalization for approximate quantification, gave the following weight percentages: 85.32% methanol, 9.66% 2-pentylnon-2-enal, 5.02% (balance) unidentified species. GC analysis of the undistilled organic phase using the same method showed 0.18% methanol, 0.79% unreacted n-heptanal, 95.39% 2-pentylnon-2-enal, and 3.64% (balance) unidentified species. The distilled organic product showed ≥98% 2-pentylnon-2-enal and ≤2% (balance) higher boiling species. Positive identification of the C_{14} alkenal was obtained by GC/MS in the Monsanto Physical Sciences Center.

Once optimum heterogeneous catalysts and reaction conditions were defined during the intermediate stages of the experimental program, other reaction product materials were prepared in reasonably high (≥99%) purity for use in developing internal standard response factors and
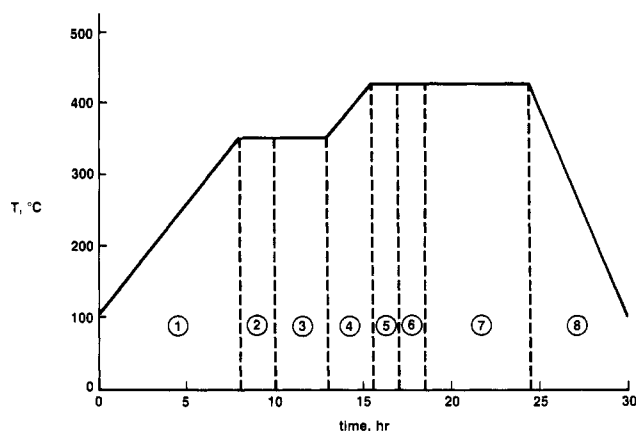

Figure 4. Temperature versus time program used for catalyst activation.

related applications. Preparation of the saturated aldehyde (2-pentylnonanal) was performed by reaction of 49.9 g of 2-pentylnon-2-enal with hydrogen at 1379 kPa and 358 K using 1 g of commercially available Engelhard 5% Pd/C powered catalyst with 4 h of reaction time. The cooled reaction product was filtered to separate the liquid and was vacuum distilled at 5 Torr with a maximum distillation bottoms temperature of 378 K. GC analysis of the product using the trimethylsilyl oxime derivatization procedure described below gave the following area normalized results: 98.09% 2-pentylnonanal (syn, anti, cis, and trans forms) and 1.91% (balance) unidentified impurities. Selective hydrogenation of 2-pentylnon-2-enal to prepare the corresponding unsaturated alcohol (2-pentylnon-2-enol) and the saturated alcohol (2-pentylnonanol) was performed using experimental conditions analogous to those described in examples 1 and 3 of Barker and Forster (1984).

Hydrogen and dimethylamine were used as received from commercial sources without any further treatment. Purities of at least 99.99% and >97% were quoted by the manufacturers which was sufficient for the objectives of this work.

Catalysts. Table I gives a summary of representative commercial catalysts which were tested and their physical properties as reported by the manufacturer or measured in our laboratory using standard techniques. These classes of catalysts were selected to compare the product distribution obtained when supported noble metal and supported base metal catalysts were used as reductive amination catalysts for the reaction given by eq 3.

The Pd-on-carbon catalysts were reduced by the manufacturer and used as received without any further pretreatment. All other catalysts shown in Table I and others from other sources having similar compositions were pretreated prior to an experiment with argon and hydrogen at elevated temperatures by using a microcomputer-controlled catalyst treatment apparatus of novel design (Delk and Vävere, 1984). To briefly summarize, this device permits the user to construct a program so that the bulk form of the catalyst is treated by single-component or

**Table II. Schedule of Events Used for the Catalyst Activation Procedure**

event	description
1	start Ar flowing at 400 sccm and increase temp from 100 to 350 °C
2	hold for 2 h in flowing Ar at 350 °C to dry the catalyst
3	initiate the hydrogen flow and increase at the rate of $^1/_9$ sccm so that the flow rate after 3 h will be 20 sccm
4	ramp the catalyst bed temp from 350 to 425 °C over the next 2.5 h
5	increase the hydrogen flow from 20 to 100 sccm over the next 1.5 h at the rate of $^8/_9$ sccm
6	decrease the Ar flow rate from 400 to 10 sccm in steps of 50 sccm every 15 min over the next 1.5-h period
7	hold the catalyst bed at 425 °C with the H_2 and Ar flow rates of 100 and 10 sccm, respectively
8	increase the Ar flow from 10 to 400 sccm and turn the H_2 flow off

multicomponent gas mixtures according to a particular temperature–time schedule so that undesired overheating or sintering of the catalyst is avoided. Figure 4 gives the temperature versus time program that was used in this work. The numbers on the figure refer to various defined events for the indicated time interval and are summarized in Table II. This procedure includes the appropriate events for reducing the catalyst under carefully controled and reproducible conditions while minimizing the potential for achievement of excess temperatures by a programmed increase in hydrogen.

Analytical Methods. All reaction samples were analyzed by using two independent Varian Model 3700 gas chromatographs equipped with flame ionization detectors. Each chromatograph was set up with a different column and a particular set of conditions which are distinguished here by reference to method 1 and method 2. In both systems, helium was used as the carrier gas at a linear velocity of ca. 30 cm/s. The columns were used in the direct injection mode with narrow-bore glass inserts in the injection ports. Make-up gas (helium) was added before the flame ionization detectors at the rate of 30 cm³/s. Temperatures for the injection port and detector were maintained at 250 °C. The hydrogen and air flows to the FID's were set at 30 and 300 cm³/min as specified by the manufacturer. The FID electrometers were usually run at sensitivities of 10^{-9} or 10^{-10} A/mV. Detector signals were displayed on 1-mV full-scale strip chart recorders (Hewlett-Packard Model 7123 or Varian Model 9176). Peak areas were determined by a laboratory automation system (Hewlett-Packard Model 3353-E) where the signal integration was based on a data collection frequency of 4 Hz. Corrections to the base line were included in each method by the use of appropriate event markers.

Method 1 employed a 50 ft × 0.02 in. i.d. support-coated open-tubular (SCOT) column coated with polar Carbowax 20M. It was used to analyze neat reaction samples, i.e., those that were not subjected to a postderivatization procedure. The column was typically operated from 60 to 240 °C at a programming rate of 8 °C/min with a 10-min hold once the final temperature was achieved. Typically, 0.05 μL of sample was injected.

Method 2 used a 40 m × 0.5 mm i.d. SCOT glass capillary column coated with OV-1. It was used to analyze reaction samples that were converted to trimethylsilyl oxime derivatives using a derivatization procedure described by Willis (1983) with some modifications for this work. The particular methodology followed here is given in Appendix A. The OV-1 column was operated from 150 to 280 °C with a programming rate of 4 °C/min. A derivatized sample injection size of 0.1 μL was found to give satisfactory results.
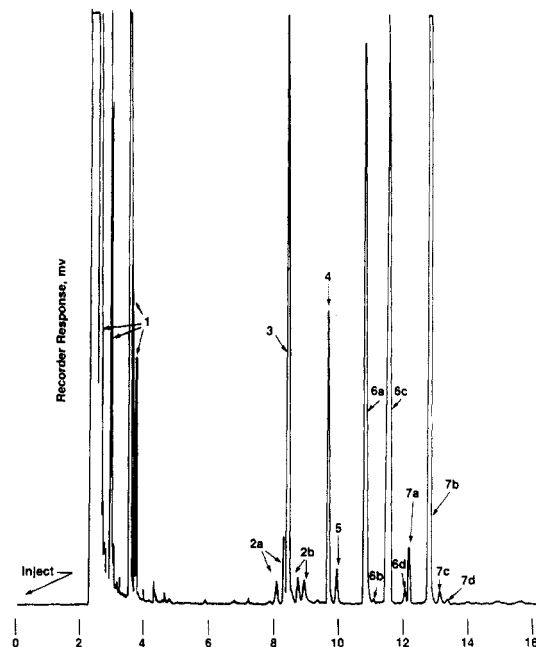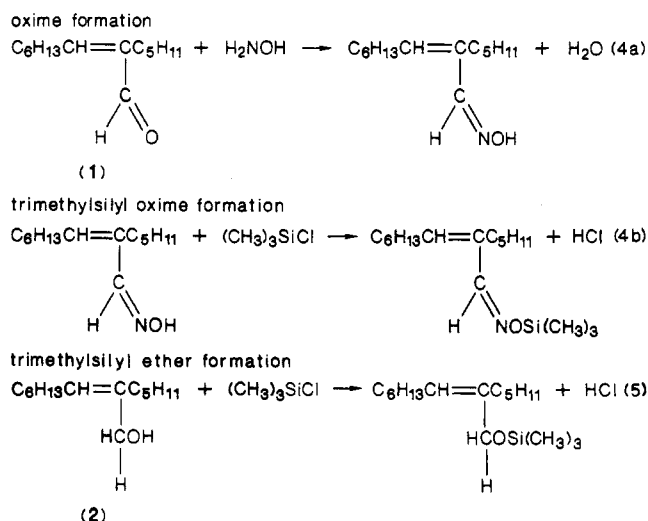

Figure 5. Chromatogram of a typical reductive amination reaction product sample obtained after application of the trimethylsilylated (TMS) oxime derivatization procedure. Identified species: 1, derivatization reagents, MeOH, and unreacted n-heptanals; 2a,b, 1-(N,N-dimethylamino)-2-pentylnon-2-ene; 3, 1-(N,N-dimethylamino)-2-pentylnonane; 4, 2-pentylnonanol; 5, 2-pentylnon-2-enol; 6a–d, 2-pentylnonanal (syn, cis, anti, and trans forms); 7a–d: 2-pentylnon-2-enal (cis, syn, anti, and trans forms). Varian 3700, 40 m × 0.5 mm i.d. SCOT OV-1 column, 150–240 °C at 4 °C/min; FID, 10^{-10} A/mV, 0.1 μL. Other parameters: 12 g of Harshaw 3210 supported nickel tablets, 115 g of 2-pentylnon-2-enal, 30 g of dimethylamine, T = 393 K, P = 3445 kPa (500 psig), t = 5 h.

Reaction Technique. A typical liquid-phase reductive amination experiment was initiated by charging between 1 and 5 g of the catalyst powder from a sealed vial to the autoclave using an argon or nitrogen purge to minimize exposure of the catalyst to air. This was followed by charging ca. 115 g of refrigerated 2-pentylnon-2-enal stored in a sealed bottle with a nitrogen headspace. The 0.3-L autoclave head was then installed and the Magne-drive purged with additional nitrogen to displace any air that might be present in the bearing support area. Hydrogen at a pressure of ca. 345 kPa was then applied and stirring was initiated for several minutes to saturate the liquid with the gas. The stirring was stopped, a leak check was performed, and then the autoclave was slowly vented to atmospheric pressure. Chilled dimethylamine was then introduced to the autoclave through the autoclave vent line from the receiver shown above in Figure 3 by applying a positive nitrogen pressure. After disconnecting the receiver, the reactor pressure was increased with hydrogen to a pressure of ca. 345 kPa. Stirring was then initiated and adjusted to 1000 rpm while power was applied to the temperature controller. Once the desired liquid batch temperature had been reached and had stabilized, additional hydrogen was quickly introduced to the reactor by adjusting the back-pressure regulator until the desired reactor pressure had been achieved. After a designated batch reaction time had elapsed (usually 4–6 h), a small sample (3–5 mL) of the reactor liquid product was collected in a chilled vial and analyzed by using the GC methods described above. In a few cases, a gas sample was collected from the autoclave head space and analyzed for fixed gases (H_2, N_2, CO, etc.) and C_1–C_5 hydrocarbons by using a Carle Series SX chromatograph.

Results and Discussion

Reaction Product Analysis. Figure 5 is a chromatogram of a typical reaction sample which was subjected to the trimethylsilyl oxime derivatization procedure as described above and analyzed on the OV-1 column. Details related to the experimental conditions are given with the figure caption.

Before proceeding, it should be noted that the derivatization procedure will result in the formation of the trimethylsilyl oxime (TO) derivatives of any aldehydes that are present in the reaction sample. In addition, the derivatization reagents will convert any byproduct alcohols to the corresponding trimethylsilyl ether derivatives. Any amines that may be present in the reaction product sample do not react with the reagents. For example, the following reactions would occur during derivatization if 2-pentylnon-2-enal (1) and 2-pentylnon-2-en-1-ol (2) were present in the sample:

oxime formation

$$C_6H_{13}CH = CC_5H_{11} + H_2NOH \rightarrow C_6H_{13}CH = CC_5H_{11} + H_2O \quad (4a)$$

(1)

trimethylsilyl oxime formation

$$C_6H_{13}CH = CC_5H_{11} + (CH_3)_3SiCl \rightarrow C_6H_{13}CH = CC_5H_{11} + HCl \quad (4b)$$

trimethylsilyl ether formation

$$C_6H_{13}CH = CC_5H_{11} + (CH_3)_3SiCl \rightarrow C_6H_{13}CH = CC_5H_{11} + HCl \quad (5)$$

(2)

Inspection of Figure 5 shows that the trimethylsilyl oxime derivatives of 2-pentylnonanal (saturated aldehyde) and 2-pentylnon-2-enal (unsaturated aldehyde) are present in this particular sample as two groups of peaks denoted by peaks 6 and 7, respectively. Since each species can exist in the form of syn, anti, cis, and trans isomers, a maximum of eight peaks is possible. For 2-pentylnonanal, two major peaks are observed at 6a and 6c with two minor peaks at 6b and 6d. For 2-pentylnon-2-enal, a major peak is observed at 7b with three minor peaks at 7a, 7c, and 7d. The unsaturated amines, which exist in both the cis and trans forms, elute between 8 and 9 min (peaks 2a and 2b) and are clustered around the desired saturated amine (peak 3). In addition to the aldehyde and amines, byproduct alcohols, such as 2-pentylnonanol (saturated alcohol) and 2-pentylnon-2-enol (unsaturated alcohol), are detected in the sample in the form of the trimethylsilyl ether derivatives in the vicinity of 10 min (peaks 4 and 5, respectively). Verification of the various species indicated on the chromatogram of Figure 5 was obtained by GC/MS using a 50-m Series 530 μ-methylsilicone column operated from 100 to 250 °C at a temperature programming rate of 8 °C/min. The precise assignment of the individual peaks obtained for a particular species to a particular isomeric form, for example, cis isomer, was not possible. However, the assignment of a group of peaks to a particular species was performed by spiking the sample with that same species. This also provided additional validation of the GC/MS results.

Figure 6 gives the chromatogram obtained when the reaction sample used to construct Figure 5 was analyzed
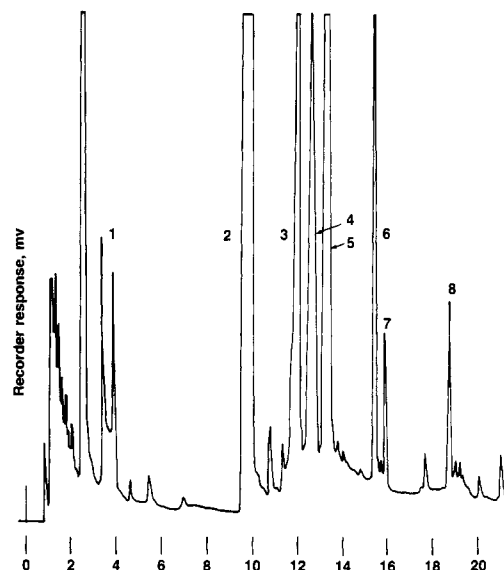
Figure 6. Chromatogram of a typical reductive amination reaction product sample without derivatization. Identified species: 1, MeOH, water, dimethylamine, and unreacted n-heptanals; 2, 1-(N,N-dimethylamino)-2-pentylnon-2-ene and 1-(N,N-dimethylamino)-2-pentylnonane; 3–5, 1-(N,N-dimethylamino)-2-pentylnon-2-enol, 1-(N,N-dimethylamino)-2-pentylnonanol, and 2-pentylnon-2-enal; 6, 7, 2-pentylnon-2-enal; 8, 2-pentylnon-2-en-1-ol. Varian 3700, 50 ft × 0.02 in. i.d. SCOT Carbowax 20M column, 60–240 °C at 8 °C/min; FID, 10^{-10} A/mV, 0.05 μL.

in an underivatized or neat form using the Carbowax 20M column corresponding above to method 1. Identification of the species associated with the major peaks 2–5 is complicated by coelution or the near coelution of the various C_{14} aldehydes with the C_{16} product amines. Inspection of Tables 6, 7, and 13–15 given in the supplementary material shows that the boiling points for the C_{14} aldehydes and C_{16} amines are within 5–10 K of each other so that coelution of these species on certain types of GC columns would be expected. Formation of the trimethylsilyl oxime and ether derivatives of the aldehydes and alcohols, respectively, leads to a greater distribution of boiling points and differences in polarity of the molecules so that chromatographic separation of these species from each other and the amines can be more readily achieved.

Other possible products that may be formed by a reaction between 2-pentylnon-2-enal and dimethylamine were investigated by GC analysis of neat autoclave samples that were removed during the heating period prior to the addition of high-pressure hydrogen. Chromatograms of these samples on the polar Carbowax 20M column showed peaks which could only be interpreted as being the isomeric products of the following reaction between 2-pentylnon-2-enal and dimethylamine:

$$C_6H_{13} = CC_5H_{11} + (CH_3)_2NH \rightleftharpoons C_6H_{13}CH = CC_5H_{11} \quad (6)$$
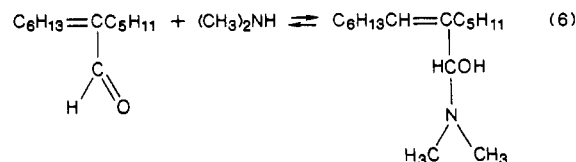
No product amines or byproduct alcohols were formed since the hydrogen pressure was apparently too low ($P \leq$ 308.2 kPa) to result in any significant solid-catalyzed reaction products. This method could not be used to obtain quantitative results for the reaction product of eq 6 after the addition of high-pressure hydrogen due to the coelution of the amines and byproduct alcohols with this product. However, it does permit identification of yet another re-

Table III. Identified Reaction Species in the Reductive Amination of 2-Pentylnon-2-enal with Dimethylamine and Various Heterogeneous Catalysts
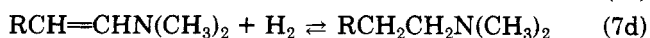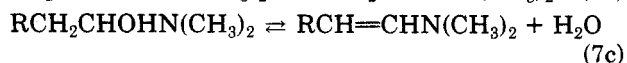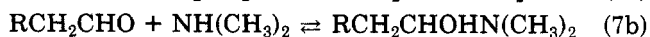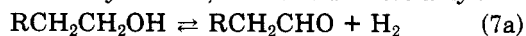
designation	formula	name
A	$C_6H_{13}CH$=$C(CHO)$-C_5H_{11}	2-pentylnon-2-enal
B	$C_6H_{13}CH_2CH(CHO)$-C_5H_{11}	2-pentylnonanal
C	$C_6H_{13}CH$=$C(CH_2OH)$-C_5H_{11}	2-pentylnon-2-en-1-ol
D	$C_6H_{13}CH_2CH(CH_2OH)$-C_5H_{11}	2-pentylnonanol
E	$C_6H_{13}CH$=$C(CHOHN$-$(CH_3)_2)C_5H_{11}$	1-(N,N-dimethylamino)-2-pentylnon-2-enol
F	$C_6H_{13}CH_2CH(CHOHN$-$(CH_3)_2)C_5H_{11}$	1-(N,N-dimethylamino)-2-pentylnonanol
G	$C_6H_{13}CH$=$C(CH_2N$-$(CH_3)_2)C_5H_{11}$	1-(N,N-dimethylamino)-2-pentylnon-2-ene
H	$C_6H_{13}CH_2C$(=CHN-$(CH_3)_2)C_5H_{11}$	1-(N,N-dimethylamino)-2-pentylnon-1-ene
I	$C_6H_{13}CH_2CH(CH_2N$-$(CH_3)_2)C_5H_{11}$	1-(N,N-dimethylamino)-2-pentylnonane
J	$NH(CH_3)_2$	dimethylamine

action intermediate which is not detected in the derivatization method because the oximation procedure forces the above adduct to the free aldehyde form.
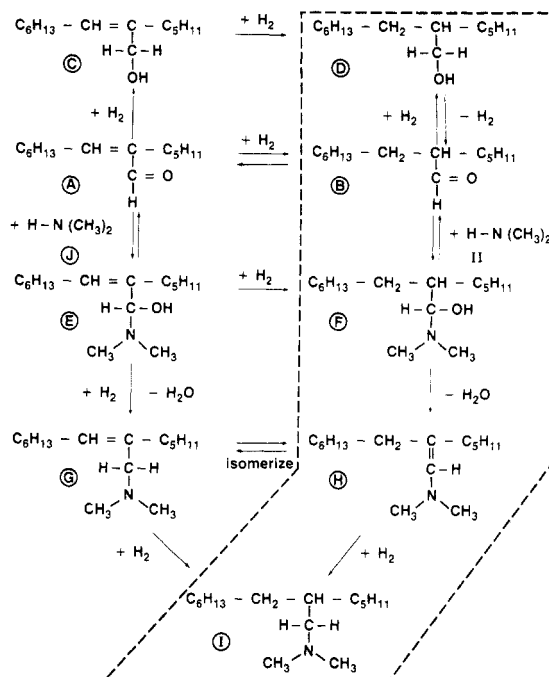
A survey of the analytical methods used to support reaction pathway and kinetic studies for reductive amination of long-chain aldehydes or alcohols, such as those reported in Baiker et al. (1983), Baiker and Kijenski (1985), and Klyuev and Khidekel (1980) and the references cited therein, shows that none of these employed GC-based derivatization techniques and relied solely on GC analysis of the neat reaction samples. While these may have been suitable in the context of these studies, our experience with the current reacting system and a few others having similar characteristics (Willis, 1983) suggests that a more complete identification of reaction species is obtained by application of the above GC analytical methods where both neat and derivatized samples are analyzed.

Amination Reaction Pathway. Table III gives a list of the various species that have been identified or speculated to be present in screening-type experiments using the catalysts presented earlier in Table I. From this list, the reaction network given in Figure 7 can be developed to explain the formation of the desired saturated amine (species I in Table III) and other various intermediates. This is self-explanatory so that a detailed description is omitted for brevity.

Reaction pathways for the reductive amination of selected long-chain alcohols, aldehydes, and ketones have been summarized in both review papers (Baiker and Kijenski, 1985; Klyuev and Khidekel, 1980) and various articles on the subject (Baiker et al., 1983; Kliger et al., 1975a,b, 1978). The work of Baiker et al. (1983) on the copper-catalyzed amination of octanol and decanol by monomethylamine and dimethylamine has characteristics that are the most closely related to the current system and provides some basis for comparison to the above results. The following pathway was set forth by Baiker et al. (1983) as being general for reactions of primary and secondary alcohols, aldehydes, and ketones with ammonia and primary and secondary amines, where R denotes alkyl.

$$RCH_2CH_2OH \rightleftharpoons RCH_2CHO + H_2 \qquad (7a)$$

$$RCH_2CHO + NH(CH_3)_2 \rightleftharpoons RCH_2CHOHN(CH_3)_2 \qquad (7b)$$

$$RCH_2CHOHN(CH_3)_2 \rightleftharpoons RCH=CHN(CH_3)_2 + H_2O \qquad (7c)$$

$$RCH=CHN(CH_3)_2 + H_2 \rightleftharpoons RCH_2CH_2N(CH_3)_2 \qquad (7d)$$

If one replaces RCH_2 in eq 7b by $C_6H_{13}CH_2CHC_5H_{11}$ and

Figure 7. Reaction network for the reductive amination of 2-pentylnon-2-enal (species A) with dimethylamine and hydrogen. The reactions in the dashed region represent a special case of those suggested by Baiker et al. (1983).

follows the development given by eq 7c and 7d using this 2-branched alkyl group, then the resulting sequence of reactions will exactly correspond to those reactions within the dashed region of Figure 7. The reaction network given in Figure 7 represents both an independent confirmation of the Baiker et al. (1983) reaction pathway and an extension of the pathway given by eq 7a–7d to reductive amination of unsaturated, branched species.

Reaction Thermodynamics. The equilibrium constants for each of the reactions given in the reaction network of Figure 7 were evaluated to determine whether or not the formation of any particular reaction products might be equilibrium limited. This was performed using a special purpose computer program called RXTHERM that has the capability of evaluating the heat of reaction, entropy of reaction, Gibbs free energy of reaction, and equilibrium constant as a function of temperature for a single chemical reaction of the form $\sum_i^s \alpha_i A_i = 0$ where α_i denotes the stoichiometric coefficient of species A_i and s denotes the total number of reacting species. The thermodynamic equations used in the program to evaluate the above quantities are well-known and are available in standard texts so that they will not be repeated here (cf. Balzhiser et al. (1972), Hougen et al. (1959), and Smith and Van Ness (1975)). Benson's contribution of groups method (Benson et al., 1969) was used to evaluate the ideal gas heat capacity, enthalpy of formation, and entropy at the standard state for each species listed in Table III from which the entropy of formation and Gibbs free energy of the ideal gas was evaluated. A combination of experimental measurements and correlating equations which are described in a related publication (Mills et al., 1987) was used to evaluate the saturated liquid properties for each of the C_{14} and C_{16} reacting species so that the ideal-gas results could be transformed to liquid-phase thermodynamics. Some typical results are given in Table IV. Tables 1–27 in the supplementary material contain the numerical values for the thermodynamic quantities for this evaluation.

A comparison of the equilibrium constants for each reaction in the network is given in Table V at temperatures

Table IV. Ideal Gas Enthalpy of Formation, Entropy, Entropy of Formation, Free Energy of Formation, and Heat Capacities for Reductive Amination Reaction Intermediates

no.	name	$\Delta H_f{}^{\circ}{}_{298},{}^{a}$ kcal mol^{-1}	$S^{\circ}{}_{298},{}^{b}$ cal mol^{-1} K^{-1}	$\Delta S_f{}^{\circ}$, cal mol^{-1} K^{-1}	$\Delta G_f{}^{\circ}$, kcal mol^{-1}	$C_p{}^{\circ}$, cal mol^{-1} K^{-1}, at					
						300 K	400 K	500 K	600 K	800 K	1000 K
1	2-pentylnon-2-enal	−77.04	190.70	−258.57	0.0526	74.76	94.76	112.03	126.98	150.34	167.64
2	2-pentylnonanal	−98.96	172.21	−308.21	−7.07	80.62	100.61	118.12	132.97	157.08	174.77
3	dimethylamine	−4.50	65.59	−69.25	16.15	16.58	28.89	24.93	28.41	33.94	38.19
4	1-(N,N-dimethylamino)-2-pentylnon-2-enol	−84.14	199.13	−384.98	30.64	93.37	118.59	141.06	159.37	187.88	208.57
5	1-(N,N-dimethylamino)-2-pentylnonanol	−108.02	199.75	−415.57	15.88	96.78	122.19	145.16	164.30	194.23	216.04
6	2-pentylnon-2-en-1-ol	−89.20	177.46	−303.02	1.15	77.03	98.02	116.65	132.27	156.59	174.49
7	2-pentylnonanol	−115.16	178.83	−332.86	−15.92	81.24	102.48	121.59	137.79	163.18	181.93
8	1-(N,N-dimethylamino)-2-pentylnon-2-ene	−46.76	188.68	−370.93	63.83	89.15	113.74	135.69	154.10	182.72	203.70
9	1-(N,N-dimethylamino)-2-pentylnonane	−71.52	190.00	−400.82	47.98	93.03	118.32	140.98	160.07	189.74	211.54
10	1-(N,N-dimethylamino)-2-pentylnon-1-ene	−43.31	188.30	−371.31	67.39	86.54	111.25	133.50	152.22	181.37	202.62

$^{a}\Delta H_f{}^{\circ}{}_{298} = \sum_{i=1}^{n}\nu_i(\Delta H_f{}^{\circ}{}_{298})_i$ + corrections. $^{b}S^{\circ}{}_{298} = \sum_{i=1}^{n}\nu_i(S^{\circ}{}_{298})_i - R$ in $\sigma_t + R \ln \eta$.

Table V. Equilibrium Constants for the Individual Reactions in the Proposed Reaction Pathway for the Reductive Amination of 2-Pentylnon-2-enal with Dimethylamine To Produce 1-(N,N-Dimethylamino)-2-pentylnonane

no.	reaction	equilibrium constants at		
		333.15 K	373.15 K	573.15
1	$C_6H_{13}CH{=}C(CHO)C_5H_{11}(1) + H_2(g) \rightarrow C_6H_{13}CH{=}C(CH_2OH)C_5H_{11}(1)$	9.324×10^{-1}	4.478×10^{-2}	1.103×10^{-5}
2	$C_6H_{13}CH{=}(CH_2OH)C_5H_{11}(1) + H_2(g) \rightarrow C_6H_{13}CH_2CH(CH_2OH)C_5H_{11}(1)$	3.265×10^{10}	4.320×10^{8}	1.553×10^{3}
3	$C_6H_{13}CH_2CH(CHO)C_5H_{11}(1) + H_2(g) \rightarrow C_6H_{13}CH_2CH(CH_2OH)C_5H_{11}(1)$	9.120×10^{6}	2.264×10^{5}	7.776×10^{0}
4	$C_6H_{13}CH{=}C(CHO)C_5H_{11}(1) + H_2(g) \rightarrow C_6H_{13}CH_2CH(CHO)C_5H_{11}(1)$	3.341×10^{3}	8.546×10^{1}	2.201×10^{-3}
5	$C_6H_{13}CH{=}C(CHO)C_5H_{11}(1) + NH(CH_3)_2(1) \rightarrow C_6H_{13}CH{=}C(CHOHN(CH_3)_2)C_5H_{11}(1)$	1.162×10^{-7}	3.379×10^{-8}	2.402×10^{-9}
6	$C_6H_{13}CH_2CH(CHO)C_5H_{11}(1) + NH(CH_3)_2(1) \rightarrow C_6H_{13}CH_2(CHOHN(CH_3)_2)C_5H_{11}$ (1)	5.120×10^{-2}	1.042×10^{-2}	$1.838 \times 10^{-3}{}^{a}$
7	$C_6H_{13}CH{=}C(CHOHN(CH_3)_2)C_5H_{11}(1) + H_2(g) \rightarrow$ $C_6H_{13}CH{=}C(CH_2N(CH_3)_2)C_5H_{11}(1) + H_2O(1)$	3.126×10^{45}	9.288×10^{38}	1.410×10^{20}
8	$C_6H_{13}CH{=}C(CHOHN(CH_3)_2C_5H_{11}(1) + H_2(g) \rightarrow C_6H_{13}CH_2CH(CHOHN(CH_3)_2)C_5H_{11}(1)$	1.472×10^{9}	2.635×10^{7}	2.119×10^{2}
9	$C_6H_{13}CH_2CH(CHOHN(CH_3)_2)C_5H_{11}(1) \rightarrow C_6H_{13}CH_2C(=CHN(CH_3)_2)C_5H_{11}(1) + H_2O(1)$	4.977×10^{9}	2.861×10^{8}	3.577×10^{4}
10	$C_6H_{13}CH{=}C(CH_2N(CH_3)_2)C_5H_{11}(1) \rightarrow C_6H_{13}CH_2C(=CHN(CH_3)_2)C_5H_{11}(1)$	4.957×10^{-3}	8.472×10^{-3}	3.561×10^{-2}
11	$C_6H_{13}CH{=}C(CH_2N(CH_3)_2)C_5H_{11}(1) + H_2(g) \rightarrow C_6H_{13}CH_2CH(CH_2N(CH_3)_2)C_5H_{11}(1)$	6.513×10^{9}	1.044×10^{8}	6.494×10^{2}
12	$C_6H_{13}CH_2C(=CHN(CH_3)_2)C_5H_{11}(1) + H_2(g) \rightarrow C_6H_{13}CH_2CH(CH_2N(CH_3)_2)C_5H_{11}(1)$	1.314×10^{12}	1.233×10^{10}	1.823×10^{4}
13	$C_6H_{13}CH{=}C(CHO)C_5H_{11}(1) + 2H_2(g) + NH(CH_3)_2(1) \rightarrow$ $C_6H_{13}CH_2CH(CH_2N(CH_3)_2)C_5H_{11}(1) + H_2O(1)$	8.296×10^{14}	1.304×10^{11}	1.711×10^{0}

^{a}At $T = 433.15$ K.

of 333, 373, and 573 K (60, 100, and 300 °C, respectively). Results for other temperatures in this range are given in Tables 29–41 in the supplementary material. The reactions involving the addition of hydrogen across a carbon–carbon double bond (reactions 2, 4, 8, 11, and 12), or formation of a saturated alcohol by hydrogenation of an aldehyde functionality (reaction 3), have large equilibrium constants. Increasing the temperature over the range of 333–573 K causes the equilibrium constants for these hydrogenation reactions to decrease by as much as 8 orders of magnitude (cf. reaction 12), but the resulting equilibrium constants at the lower temperatures are large enough that the reactions may be considered to be irreversible. Hydrogenation of the unsaturated aldehyde to the unsaturated alcohol (reaction 1) has equilibrium constants that are several orders of magnitude less than the remaining hydrogenation reactions. The numerical values suggest that this reaction may be considered reversible at the higher temperatures.

The above results for the hydrogenation reactions suggest that any catalyst which results in alcohol formation at low to moderate temperatures is not preferred since conversion of the alcohol to the aldehyde intermediate is equilibrium limited. At higher temperatures, the equilibrium constant for the alcohol conversion to the aldehyde is more favorable, but thermal stability measurements have shown (Mills et al., 1987) that 2-pentylnon-2-enal decomposes at temperatures in excess of 500–510 K. A catalyst that selectively hydrogenates the internal carbon–carbon double bond of the 2-alkenals at low-to-moderate temperatures appears to be necessary to obtain maximum selectivity to the desired saturated amine in this application.

Additional examination of Table V shows that the equilibrium constants for addition of dimethylamine to 2-pentylnon-2-enal and 2-pentylnonanal according to reactions 5 and 6, respectively, ranges from 2 × 10^{-9} to 5 × 10^{-2}. Consequently, these reactions may be considered reversible and could possibly exist at equilibrium during the reaction. The products of these reactions undergo either dehydration in reactions 7 and 9, where water is formed as a product, or hydrogenation in reaction 8. Chilled reaction samples removed from the autoclave during the course of an experiment provided direct evidence for these reactions since water was noted to be present as an immiscible lower liquid layer in the sample vial.

Isomerization or migration of the carbon–carbon double bond in the unsaturated amine is described by reaction 10. The equilibrium consant for this reaction indicates that formation of the 2-ene species is favored over the 1-ene species, but this decreases with increasing temperature. The magnitude of the equilibrium constant is not overwhelmingly large over the indicated temperature range so that liquid-phase isomerization might occur with the appropriate catalyst.

Although the above thermodynamic results were specifically developed for 2-pentylnon-2-enal, the results are also valid for each of the remaining 27 C_{14} 2-alkenal isomers that would be present in an isomeric mixture of hexenes was used in eq 1. A tabulation of these isomers and the saturated amines that would be derived from these according to the reaction stoichiometry given earlier by eq 3 is provided in Tables I and II of a related paper (Mills et al., 1987). If all of these isomers were present in the reaction mixture, then application of the reaction pathway

Table VI. Key Catalyst Screening Results

catalyst	catalyst form	exptl conditions	$X_A{}^b$	$S_B{}^c$	$S_C{}^d$	$S_D{}^e$	$S_G{}^f$	$S_I{}^g$
Engelhard 5% Pd/C	powder	3551 kPa, 363 K, 120 min	97	19.5	0	0	10.2	70.3
Calsicat CuO/CuCr$_2$O$_4$ E-106TR	powder	6998 kPa, 423 K, 240 min	100	0	36.7	8.5	41.8	13
UCI Co/Kieselguhr	powder	6998 kPa, 423 K, 240 min	100	0	17.8	50.1	10.2	21.8
Harshaw Co-0164	tablets 3.2 mm × 3.2 mm	3551 kPa, 393 K, 300 min	6.98	71.6	8.5	10.2	9.7	0
Harshaw Ni-3210	powder	6998 kPa, 423 K, 360 min	97.4	38.1	1.0	8.5	5.6	46.8
Harshaw Ni-3210	tablets 3.2 mm × 3.2 mm	3551 kPa, 363 K, 360 min	30.9	71	0	4.8	8.2	16
Harshaw Ni-3210	tablets 3.2 mm × 3.2 mm	3551 kPa, 393 K, 360 min	33	20.7	2.7	14.9	9.9	51.8

^{a} Typical initial charge: 115 g of 2-pentylnon-2-enal, 30.2 g of dimethylamine, 1 g of catalyst for powder runs, 12 g of catalyst for tablet runs. ^{b} % conversion of 2-pentylnon-2-enal. ^{c} % selectivity to 2-pentylnonanal. ^{d} % selectivity to 2-pentylnon-2-en-ol. ^{e} % selectivity to 2-pentylnonanol. ^{f} % selectivity to 1-(N,N-dimethylamino)-2-pentylnon-2-ene. ^{g} % selectivity to 1-(N,N-dimethylamino)-2-pentylnonane.

given in Table V would lead to a set of $12 \times 28 = 336$ simultaneous chemical reactions. Fortunately, the terminal alkyl groups C_6H_{13} and C_5H_{11} lead to similar values for the Gibbs free energy so that the thermodynamic results developed here for a single isomer are similar to those that would be obtained for the remaining isomers. The use of the single isomer as a model compound to examine the reaction network and reaction thermodynamics has a definite advantage in this case.

Catalyst Screening Results. Table VI gives a summary of the key results obtained when the catalysts given earlier in Table I were evaluated in screening-type tests. The objective in this case was to identify which catalyst provided the highest conversion of 2-pentylnon-2-enal (species A in Table III) with the maximum selectivity to the unsaturated and saturated amines (species G, H, and I in Table III) at mild reaction temperatures and hydrogen pressures. An examination of the results shows that the Pd-on-carbon powder gave an overall 2-pentylnon-2-enal conversion of 97% while providing a combined unsaturated and saturated amine selectivity of 80.5% with 19.5% selectivity to the 2-pentylnonanal. At the given temperature and hydrogen pressure (i.e., 363 K and 3551 kPa), formation of either the unsaturated or saturated alcohols did not occur with this catalyst. This was independently confirmed by separate hydrogenation experiments performed at identical reaction conditions but in the absence of dimethylamine where it was noted that only the saturated aldehyde 2-pentylnonanal was obtained as a reaction product.

The base metal catalysts gave varying degrees of both unsaturated and saturated alcohol byproduct formation which resulted in lower selectivities to the desired unsaturated and saturated amines. Generally, these required higher temperatures and hydrogen pressures and longer reaction times to obtain the same degree of unsaturated aldehyde conversion when compared to the Pd-on-carbon noble metal catalyst. When commercially available catalyst tablets were used in the spinning catalyst basket, conversion of the 2-pentylnon-2-enal was significantly less than that obtained with the powdered catalysts for the same batch reaction time. Also, different reaction product selectivities were obtained. This result is not surprising since internal diffusion limitations were estimated to be present with the tablet catalysts, although precise values for the effectiveness factors were not determined. A series–parallel system of reactions in a catalyst pellet with internal diffusion limitations would naturally lead to different values of product selectivity when compared to an equivalent loading of catalyst powder whose effectiveness factor was nearly unity.

While the base metal catalysts are less costly than the noble metal Pd-on-carbon catalyst on a per pound basis, they lead to inferior amine product selectivities and require more severe reaction conditions. Therefore, they are not recommended for this application. This result differs from

the one obtained by Baiker et al. (1983) who showed that supported copper catalysts are capable of reductively aminating long-chain alcohols with monomethylamine or dimethylamine to the corresponding long-chain amine in high selectivity. The key difference here is that the conversion of the alcohol to an aldehyde intermediate was identified as the rate-determining step, whereas the current application employs aldehydes as the starting reactant which is not necessarily rate-determining.

Reaction Kinetics. Interpretation of concentration versus time data obtained from various batch autoclave experiments was also performed using the reaction network given in Figure 7 as the basis. The objective in this case was not to perform a complete intrinsic kinetics study but to provide a starting basis for a more detailed future kinetics investigation where the 2-pentylnon-2-enal model compound used in this work was replaced by a typical pilot-plant feed mixture that contained all of the C_{14} 2-alkenal isomers (Mills et al., 1988). The kinetic data given here were collected using the Pd-on-carbon catalyst since the screening experiments demonstrated that this system gave the highest selectivity to the desired saturated amines with no significant byproduct formation. Preliminary experiments were performed in which agitator speed, mean catalyst powder diameter, and catalyst loading were varied to ensure that the measured bulk concentrations corresponded to intrinsic kinetics so that corrections for external mass-transfer resistances or internal particle pore diffusional resistances were not necessary. Catalyst loadings that did not exceed 7×10^{-3} g/g with a maximum mean particle size of 48.5 μm at stirring speeds of ca. 1200 rpm were identified as being appropriate for obtaining intrinsic data at temperatures of less than 373 K with hydrogen pressures between 3551 and 13 893 kPa absolute.

Figure 8 is a generalized representation of the reaction network given in Figure 7 where the species A, B, ..., I correspond to those given earlier in Table III. The assignment of irreversible and reversible reactions is based upon the reaction thermodynamic equilibrium constants given in an earlier section. With the above assumptions, the mass balance equation for the batch autoclave reduces to the following coupled system of differential equations for the case of constant liquid density which is a good approximation in this work:

$$-d\boldsymbol{u}/dt = \mathbf{K}\boldsymbol{u} \qquad (8)$$

The vector $\boldsymbol{u}$ corresponds to the liquid-phase concentrations of the various C_{14} and C_{16} species listed earlier in Table III, while $\mathbf{K}$ denotes a 9×9 matrix of kinetic constants that are associated with the reactions given in Figure 8 (Chart I). The initial condition for eq 8 is

$$\text{at } t = 0, \qquad \boldsymbol{u} = \boldsymbol{u}_0 \qquad (9)$$

Equation 8 is based upon the assumption that the intrinsic reaction rates exhibit a first-order or pseudo-first-order dependence on the liquid reactant. This rep-

Chart I. Matrix of Kinetic Constants

$$K = \begin{bmatrix} k_1 + k_4 & -k_{-4} & 0 & 0 & 0 & 0 & 0 & 0 & 0 \\ -k_4 & k_{-4} + k_6 & 0 & 0 & 0 & -k_{-6} & 0 & 0 & 0 \\ -k_1 & 0 & 0 & 0 & 0 & 0 & 0 & 0 & 0 \\ 0 & -k_3 & -k_2 & 0 & 0 & 0 & 0 & 0 & 0 \\ -k_5 & 0 & 0 & 0 & k_{-5} + k_7 + k_8 & 0 & 0 & 0 & 0 \\ 0 & -k_6 & 0 & 0 & 0 & k_{-6} + k_9 & 0 & 0 & 0 \\ 0 & 0 & 0 & 0 & -k_7 & 0 & k_{10} + k_{11} & -k_{-10} & 0 \\ 0 & 0 & 0 & 0 & 0 & -k_9 & -k_{10} & k_{-10} + k_{12} & 0 \\ 0 & 0 & 0 & 0 & 0 & 0 & -k_{11} & -k_{12} & 0 \end{bmatrix}$$
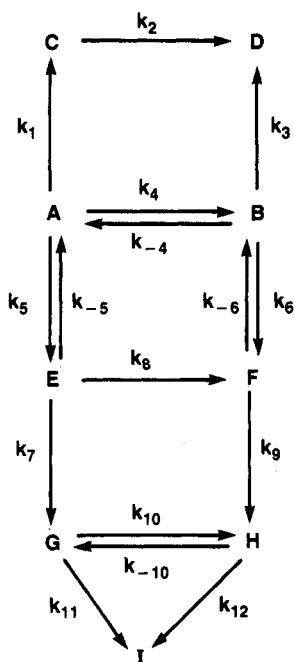
Figure 8. Generalized form of the reaction network for interpretation of the reaction kinetics.

Figure 9. Experimental and model-predicted species concentrations versus reaction time for the reductive amination of 2-pentylnon-2-enal. Catalyst, 5% Pd-on-carbon; catalyst loading, 6.9 × 10⁻³ g/g; initial charge, 115 g of 2-pentylnon-2-enal, 30.2 g of dimethylamine; pressure, 3551 kPa of hydrogen; temperature, 363 K; species, (●) 2-pentylnon-2-enal; (■) 2-pentylnonanal; (△) 2-pentylnon-2-en-1-ol; (⊠) 1-(N,N-dimethylamino)-2-pentylnon-2-ene; (○) 1-(N,N-dimethylamino)-2-pentylnonane. Predicted values are denoted by the lines.

resents a reasonable assumption for the reactions involving dimethylamine and either 2-pentylnon-2-enal or 2-pentylnonanal (cf. reactions 5 and 6 in Table V) since the dimethylamine was initially present in a 20% molar excess. In addition, independent studies performed with these substrates at different initial substrate concentrations with the Pd-on-carbon catalyst in the absence of dimethylamine have shown that hydrogen reduction of the internal carbon–carbon double bond exhibits pseudo-first-order behavior with respect to the substrate. Finally, qualitative examination of the concentration versus time data suggested exponential-type function behavior which is indicative of first-order systems.

Methods for identifying the unknown kinetic rate constants in the matrix **K** from experimental data for linear systems that are described by eq 8 and 9 have been recently reviewed by Christoffel (1982). These include the now-classical Wei–Prater (1962) method of kinetic analysis, an alternate approach proposed by Gavalas (1973), and kinetic parameter estimation by the application of optimization procedures (Bard, 1974; Froment, 1975). The latter approach was used in this work. The vector of unknown rate constants *k* that appear in the matrix **K** was obtained by minimization of the following objective function:

$$\phi = \sum_{i=1}^{n} w_i (u_{i,\text{exp}} - u_{i,\text{mod}})^2 \tag{10}$$

The variable n in the above equation denotes the number of experimental points. The subscript exp denotes the experimental values for the species concentrations, and the
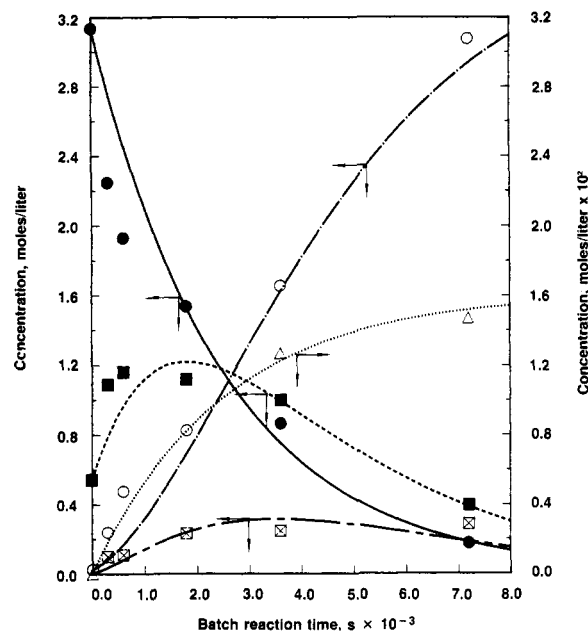
subscript mod represents the model-predicted values. The minimization of ϕ was performed by using a modified form of the BSOLVE computer program given by Kuester and Mize (1973) which is based upon Marquardt's method (Marquardt, 1970). Order of magnitude initial estimates for some of the kinetic constants were performed by using point values of the rate obtained by differentiation of the experimental concentration versus time data.

Figure 9 gives a typical comparison between the experimental data and model-predicted values for the species concentrations. The concentration of the unsaturated aldehyde 2-pentylnon-2-enal (denoted by ●) steadily decreases while the saturated aldehyde 2-pentylnonanal (denoted by ■) increases until a maximum in concentration is obtained at which point it slowly decreases as it reacts further to produce nitrogen-bearing products. Hydrogenation of the unsaturated aldehyde to the unsaturated alcohol 2-pentylnon-2-en-1-ol occurs (denoted by △, corresponding to the secondary y axis), but the maximum concentration for the alcohol is nearly 2 orders of magnitude less than the maximum concentration achieved by the saturated aldehyde (y-axis label on the right). Hydrogenation of the unsaturated alcohol to the saturated alcohol 2-pentylnonanol does not occur for the reaction conditions given on the figure for this catalyst so that the reaction rate constants $k_2 = k_3 = 0$. The minute amount

Table VII. Estimated Kinetic Parameters for the Reductive Amination of 2-Pentylnon-2-enal with Dimethylamine and Hydrogen[a]

parameter	estd value	parameter	estd value
k_1	2.0405×10^{-6}	k_{-6}	1.0785×10^{-1}
k_2	0	k_7	0
k_3	0	k_8	0
k_4	3.9651×10^{-4}	k_9	4.7652×10^{-2}
k_{-4}	2.0031×10^{-6}	k_{10}	5.4481×10^{-4}
k_5	0	k_{-10}	1.2397
k_{-5}	0	k_{11}	3.7491×10^{-4}
k_6	1.6109×10^{-3}	k_{12}	1.6257

[a] Reaction conditions: Engelhard 5% Pd/C catalyst; temperature = 363 K; hydrogen pressure = 3551 kPa (absolute); initial charge, 2-pentylnon-2-enal = 115 g, dimethylamine = 30.2 g, catalyst powder = 6.9×10^{-3} g.

of unsaturated alcohol that is formed and the lack of any detectable presence of saturated alcohol shows that Pd-on-carbon exhibits little or no potential for hydrogen addition to the aldehyde functionality for this system at these conditions. This is an important feature if high selectivity to the desired product amines is desired at mild reaction conditions.

Additional examination of Figure 9 shows that both the unsaturated amine 1-(N,N-dimethylamino)-2-pentylnon-2-ene (denoted by ⊠) and the saturated amine 1-(N,N-dimethylamino)-2-pentylnonane (denoted by ○) steadily increase with increasing reaction time. The internal double bond of the unsaturated amine is readily hydrogenated by the Pd-on-carbon catalyst to the desired amine since the relative concentration ratio of saturated amine to unsaturated amine is significantly greater than unity. The ability of the catalyst to selectively hydrogenate the internal carbon–carbon double bond in the unsaturated amine would be expected in view of the earlier results where hydrogenation of the unsaturated aldehyde to the saturated aldehyde was noted. Numerical values for the kinetic constants are given in Table VII.

Evaluation of the reaction rate for the unsaturated aldehyde 2-pentylnon-2-enal is also of interest for comparison to literature data on alcohol amination. Evaluating the rate using the data given on Figure 9 at $t = 0$ gives $r = 1.5 \times 10^{-3}$ kmol/(kg·s) where the units have been converted to agree with those of Baiker et al. (1983). These authors report a reaction rate of 5×10^{-5} kmol/(kg·s) in Figure 4 of their paper for the amination of octanol by dimethylamine at $C_{oct} = 3.0$ kmol/m^3 using Cu/alumina catalyst at $T = 483$ K. This reaction rate is nearly 2 orders of magnitude less than the one obtained here while the temperature is nearly 120 K greater. These differences between the intrinsic reaction rate are believed to be due to differences in the lower inherent activity of the supported copper compared to the supported palladium used here, as well as differences between the concentrations of adsorbed reaction species that exist on the catalyst surfaces. In addition, conversion of the alcohol to an aldehyde represents an additional reaction step when compared to the case encountered here where the aldehyde is already present.

Summary and Conclusions

Reductive amination of a novel class of long-chain substituted alkenal isomers has been studied by use of a single isomer whose reactive functional groups are identical with the remaining isomers. Supported palladium-on-carbon is the most effective catalyst for the simultaneous saturation of the internal carbon–carbon double bond and for addition of dimethylamine to the aldehyde functionality to produce unsaturated and saturated amine products

in high selectivity. Although supported base metal catalysts have been shown in previous work to be useful for the reductive amination of long-chain alcohols, ketones, and related molecules, these catalysts lead to lower amine product selectivity with significantly lower intrinsic reaction rates for the class of long-chain alkenals encountered in this work.

The reaction pathway for the reductive amination of the selected alkenal isomer with dimethylamine is complex. It involves the simultaneous hydrogenation of internal carbon–carbon double bonds, selective addition of dimethylamine to the aldehyde functionality, and the possibility of internal double-bond migration. The addition of dimethylamine to the unsaturated and saturated aldehydes, hydrogenation of the unsaturated and saturated aldehydes, and the double-bond migration are reversible reactions. All other reactions in the network are irreversible based upon thermodynamic considerations. Interpretation of kinetic data for the reaction network using integrated reaction rate expressions that are based upon first-order or pseudo-first-order behavior gives good agreement between experimental and model-predicted values for the species concentrations. Use of palladium-on-carbon catalysts for the reductive amination of an isomeric mixture of long-chain alkenals and interpretation of kinetic data using the approach outlined here now seems possible.

Acknowledgment

Nomenclature

A = concentration of 2-pentylnon-2-enal, mol cm^{-3}

A_i = concentration of species i appearing after eq 6, mol cm^{-3}

B = concentration of 2-pentylnonanal, mol cm^{-3}

C = concentration of 2-pentylnon-2-en-1-ol, mol cm^{-3}

D = concentration of 2-pentylnonanol, mol cm^{-3}

E = concentration of 1-(N,N-dimethylamino)-2-pentylnon-2-enol, mol cm^{-3}

F = concentration of 1-(N,N-dimethylamino)-2-pentylnonanol, mol cm^{-3}

G = concentration of 1-(N,N-dimethylamino)-2-pentylnon-2-ene, mol cm^{-3}

H = concentration of 1-(N,N-dimethylamino)-2-pentylnon-1-ene, mol cm^{-3}

I = concentration of 1-(N,N-dimethylamino)-2-pentylnonane, mol cm^{-3}

J = concentration of dimethylamine, mol cm^{-3}

k = first-order or pseudo-first-order rate constant appearing in Table VII and Chart I, s^{-1}

$\mathbf{K}$ = matrix of kinetic constants defined by Chart I

n = number of experimental time points versus experimental concentration data points appearing in eq 10

t = reaction time, s

$\boldsymbol{u}$ = vector of species concentrations first appearing in eq 8, mol cm^{-3}

$\boldsymbol{u}_0$ = vector of initial species concentration appearing in eq 9, mol cm^{-3}

w_i = weight associated with the ith experimental point appearing in eq 10

Greek Symbols

α_i = denotes the stoichiometric coefficient for species i

ϕ = objective functive defined by eq 10, mol^2 cm^{-6}

Subscripts

exp = denotes an experimental data point
i = denotes the ith experimental point
mod = denotes the model-predicted value

Appendix A. Description of the Sample Derivatization Procedure

Reaction samples collected from the reductive amination experiments were typically based upon an initial 2-pentylnon-2-enal concentration of about 80 wt % and an initial dimethylamine concentration of 20 wt %. A 100-μL aliquot of the sample was pipeted into a 2-mL vial using a Lacer micropipet with disposable tips. To this was added a 200-μL aliquot of a hydroxylamine hydrochloride solution. This latter solution was prepared by addition of hydroxylamine hydrochloride crystals ($H_2NOH \cdot HCl$, Fisher Scientific reagent grade) to pyridine to yield a solution concentration of 100 mg/mL. The above aliquot of hydroxylamine hydrochloride solution was selected to ensure that a stoichiometric excess of the hydroxylamine existed when compared to the maximum expected concentration of C_{14} aldehydes and alcohols in the reaction sample aliquot. The vial was then capped with a Teflon-lined septum, shaken to mix the contents, and placed in a 60 °C heated block for 5 min or until the solution had a homogeneous appearance after mixing. The sample was then removed from the block and 300–500 μL of silylation reagent was added. The reagent used was BSTFA plus 10% TMCS (Regis Chemical). This solution was then heated at 60 °C for 5 min and at 100 °C for an additional 5 min or until the solution was homogeneous after mixing. After removing the derivatized sample from the block and cooling, it was injected as described in the text according to method 2.

Registry No. A, 3021-89-4; B, 88015-71-8; C, 14466-08-1; D, 5333-48-2; E, 114184-38-2; F, 114184-39-3; G, 99916-29-7; H, 114184-40-6; I, 99916-30-0; J, 124-40-3; Pd, 7440-05-3; Ni, 7440-02-0; Co, 7440-48-4; Cu, 7440-50-8; Cr, 7440-47-3; Ba, 7440-39-3.

Supplementary Material Available: Tables 1–5 listing group contribution data, Tables 6–15 listing calculated saturated liquid–gas properties, and Tables 16–54 listing reaction thermodynamics for the compounds mentioned in the text (66 pages). Ordering information is given on any current masthead page.

Literature Cited

Baiker, A.; Kijenski, J. *Catal. Rev.-Sci. Eng.* **1985**, *27*, 653.

Baiker, A.; Caprez, W.; Holdstein, W. L. *Ind. Eng. Chem. Prod. Res. Dev.* **1983**, *22*, 217.

Balzhiser, R. E.; Samuels, M. R.; Eliassen, J. D. *Chemical Engineering Thermodynamics*; Prentice-Hall: Englewood Cliffs, NJ, 1972.

Bard, Y. *Nonlinear Parameter Estimation*; Academic: New York, 1974.

Barker, G. E.; Forster, D. U.S. Patent 4 426 542, 1984.

Bathina, H. B.; Reck, R. A. In *Kirk–Othmer Encyclopedia of Chemical Technology*, 3rd ed.; Mark, H. F., Othmer, D. F., Overberger, C. G., Seaborg, G. T., Eds.; Wiley: New York, 1978; Vol. 2, pp 283–295.

Beil, W., et al. German Offen. 1 468 788, 1969.

Benson, S. W.; Cruickshank, F. R.; Golden, D. M.; Haugen, G. R.; O'Neal, H. E.; Rodgers, A. S.; Shaw, R.; Walsh, R. *Chem. Rev.* **1969**, *69*, 279.

Christoffel, E. G. *Catal. Rev.-Sci. Eng.* **1982**, *24*, 159.

Dadekian, Z. A.; Wilbourn, D. S. U.S. Patent 3 471 561, 1969.

Delk, F. S., II; Vávere, A. *J. Catal.* **1984**, *85*, 380.

Dudzinski, Z. J. U.S. Patent 3 548 001, 1970.

Dudzinski, Z. J. U.S. Patent 3 732 312, 1973.

Falbe, J., Ed. *New Synthesis with Carbon Monoxide*; Springer-Verlag: New York, 1980.

Forster, D.; Schaefer, G.; Barker, G. E. U.S. Patent 4 598 162, 1986.

Froment, G. F. *AIChE J.* **1975**, *21*, 1041.

Gavalas, G. R. *AIChE J.* **1973**, *19*, 214.

Herman, R. G. In *Catalytic Conversions of Synthesis Gas and Alcohols to Chemicals*; Herman, R. G., Ed.; Plenum: New York, 1984.

Hoshino, F.; Kimura, H.; Matsutani, K. U.S. Patent 4 210 605, 1980.

Hougen, O. A.; Watson, K. M.; Ragatz, R. A. *Chemical Process Principles*, 2nd ed.; Wiley: New York, 1959; Part II.

Imai, T. U.S. Patent 4 179 469, 1979.

Imai, T. U.S. Patent 4 207 260, 1980.

Imai, T. U.S. Patent 4 250 115, 1981.

Kimura, H.; Matsutani, K.; Tsutsumi, S. U.S. Patent 4 254 060, 1981.

Kliger, G. A.; Lazutina, L. F.; Fridman, R. A.; Kryukow, Y. B.; Bashkirov, A. N.; Snagovskii, Y. S.; Smirnova, R. M. *Kinet. Katal.* **1975a**, *16*, 660.

Kliger, G. A.; Lazutina, L. F.; Fridman, R. A.; Kryukow, Y. B.; Bashkirov, A. N.; Snagovskii, Y. S.; Smirnova, R. M. *Kinet. Katal.* **1975b**, *16*, 665.

Kliger, G. A.; Glebov, L. S.; Fridman, R. A.; Vytnova, L. A.; Bashkirov, A. N. *Kinet. Katal.* **1978**, *19*, 615.

Klyuev, M. V.; Khidekel, M. L. *Russ. Chem. Rev.* **1980**, *49*, 14.

Kraiman, E.; Austin, J. U.S. Patent 3 401 203, 1968.

Kuester, J. L.; Mize, J. H. *Optimization Techniques with Fortran*; McGraw-Hill: New York, 1973.

Marquardt, D. W. *Technometrics* **1970**, *12*, 591.

Mather, P. E., et al. British Patent 1 538 199, 1979.

McCarty, C. B., et al. German Offen 1 468 787, 1969.

Mills, P. L.; Fenton, R. L.; Schaefer, G. F. *J. Chem. Eng. Data* **1987**, *32*, 251.

Mills, P. L.; Willis, D. E.; Fenton, R. L., unpublished results, 1988.

Mueller, H., et al. French Patent 2 351 088, 1977.

Nekrasova, V. A.; Shiukin, N. I. *Russ. Chem. Rev.* **1965**, *34*, 843.

Pivette, P. U.S. Patent 3 764 626, 1973.

Rylander, P. N. *Catalytic Hydrogenation in Organic Syntheses*; Academic: New York, 1979.

Slaugh, L. H. U.S. Patent 4 206 149, 1980a.

Slaugh, L. H. U.S. Patent 4 206 150, 1980b.

Slaugh, L. H. British Patent 2 006 773, 1982.

Smith, J. M.; Van Ness, H. C. *Introduction to Chemical Engineering Thermodynamics*, 3rd ed.; McGraw-Hill: New York, 1975.

Strauss, J.; Hübner, H., Müller, H.; Krempl, E. U.S. Patent 4 138 437, 1979.

Wakeman, R. L.; Shay, E. G. U.S. Patent 3 471 562, 1969.

Wattimena, F., et al. British Patent 1 553 285, 1979.

Wei, J.; Prater, C. D. *Adv. Catal.* **1962**, *13*, 137.

Weissermel, K.; Arpe, H. J. *Industrial Organic Chemistry*; Verlag Chemie: New York, 1978.

Willis, D. E. *J. Chromatogr. Sci.* **1983**, *21*, 132.